NIH Public Access
Author Manuscript
Cardiovasc Pathol. Author manuscript; available in PMC 2013 May 01.

Published in final edited form as:
Cardiovasc Pathol. 2012 ; 21(3): 188–198. doi:10.1016/j.carpath.2011.05.002.

Variable Phenotype in Murine Transverse Aortic Constriction (TAC)

Selma F. Mohammed, **Jimmy R. Storlie**, **Elise A. Oehler**, **Lorna A. Bowen**, **Josef Korinek**, **Carolyn SP Lam**, **Robert D. Simari**, **John C. Burnett Jr.**, and **Margaret M. Redfield**
Cardiorenal Research Laboratory, Mayo Clinic, Rochester, MN

Abstract

Background—In mice, transverse aortic constriction (TAC) is variably characterized as a model of pressure overload induced hypertrophy (LVH) or heart failure (HF). While commonly used, variability in the TAC model is poorly defined. The objectives of this study were to characterize the variability in the TAC model and to define a simple, non-invasive method of prospectively identifying mice with HF versus compensated LVH after TAC.

Methods—Eight week old, male C57BL/6J mice underwent TAC or SHAM and then echo at three weeks post-TAC. A group of SHAM and TAC mice were sacrificed after the three week echocardiogram, while the remainder underwent repeat echo and sacrifice at nine weeks post-TAC. The presence of TAC was assessed with 2 dimensional echo, anatomic aortic m-mode and color flow and pulsed-wave Doppler examination of the transverse aorta (TA) and by LV systolic pressure (LVP). Trans-TAC pressure gradient was assessed invasively in a subset. HF was defined as lung/body weight > upper limit in SHAM operated mice.

Results—As compared to SHAM, TAC mice had higher TA velocity, LVP and LV weight and lower ejection fraction (EF) at three or nine weeks post-TAC. Only a subset of TAC mice (28%) developed HF. As compared to compensated LVH, HF mice were characterized by similar TA velocity and higher percent TA stenosis, but lower LVP, higher LV weight, larger LV cavity, lower EF and stress-corrected midwall fiber shortening and more fibrosis. Both EF and LV mass measured by echo at three weeks post-TAC were predictive of the presence of HF at three or nine weeks post-TAC.

Conclusions—In wild type mice, TAC produces a variable cardiac phenotype. Marked abnormalities in LV mass and EF at echo three weeks post-TAC identify mice with HF at autopsy. These data are relevant to appropriate design and interpretation of murine studies.

Keywords

Transverse aortic constriction (TAC); Pressure overload hypertrophy; Murine models; Cardiac geometry; Left ventricular hypertrophy (LVH)

© 2011 Elsevier Inc. All rights reserved.

Address for correspondence: Margaret M. Redfield, MD, Cardiovascular Research, Guggenheim 9, Mayo Clinic, 200 First Street, Southwest, Rochester, Minnesota 55905, Tel. (507) 284-1281; Fax. (507) 266-4710; redfield.margaret@mayo.edu.

Publisher's Disclaimer: This is a PDF file of an unedited manuscript that has been accepted for publication. As a service to our customers we are providing this early version of the manuscript. The manuscript will undergo copyediting, typesetting, and review of the resulting proof before it is published in its final citable form. Please note that during the production process errors may be discovered which could affect the content, and all legal disclaimers that apply to the journal pertain.

NIH-PA Author Manuscript
NIH-PA Author Manuscript
NIH-PA Author Manuscript

NIH-PA Author Manuscript

NIH-PA Author Manuscript

NIH-PA Author Manuscript

Background

Animal models of hypertensive heart disease and heart failure (HF) are vital for advancement of our understanding of the pathophysiology of these diseases and development of novel therapies (1). The murine transverse aortic constriction (TAC) model developed by Rockman et al (2) is widely used to characterize the impact of genetic or pharmacologic interventions on cardiac remodeling in mice.

Studies have utilized variable techniques for TAC and characterized changes with TAC at variable time points with variable methods and in different strains and genetic models. The cardiac phenotype of this model has been described as compensated hypertrophy (LVH) in some studies (2-5), and as HF in others (6-10). This may be a critical distinction as the presence of HF may be associated with differential activation of signaling pathways (11,12) and differential response to pharmacologic interventions (13-15). Further, variability in a model will affect the sample size required to detect the influence of genetic or pharmacologic interventions on LV structure or function and is particularly important when small subsets are selected for assessment of different hemodynamic, biochemical or genetic parameters.

Although some studies reported on variability of the TAC model explained by mouse strain or parent of origin (16,17), sex (17,18), size of needle used to standardize constriction (15,19) or time course (20,21), only a few studies reported variability independent of these aforementioned factors (13,20-23). In general, these studies were small and did not identify a method to prospectively identify the variable phenotype.

Accordingly, the aims of this study were to characterize variation in TAC (independent of mouse age, sex, strain, needle size or time course) and to develop a feasible non-invasive means to prospectively confirm the severity of TAC and to determine the presence of HF versus compensated LVH in response to TAC. Based on our preliminary observations with the model, we hypothesized that despite a standardized surgical procedure, murine TAC produces two phenotypes: compensated LVH and HF. Further, we endeavored to determine if differences in the resulting phenotype were due to variation in the degree of TA stenosis produced by the standardized TAC procedure. Finally, we sought to establish a simple non-invasive method to predict the ultimate phenotype such that mice destined to develop compensated LVH or HF could be randomized to experimental interventions in a balanced manner.

Methods

All experimental procedures were designed in accordance with the National Institute of Health guidelines and approved by Mayo Foundation Institutional Animal Care and Use Committee.

Study design

Eight week old male wild type mice of C57/BL6 background (Jackson laboratory, Bar Harbor, ME) were subjected to minimally invasive TAC or SHAM procedure, and then studied by echo at three weeks (3 wk TAC). A subgroup of SHAM (n=28) and TAC (n= 46) mice underwent hemodynamic assessment immediately after echo and was sacrificed for tissue harvest (3 wk TAC). Remaining mice (n=10 SHAM and 43 TAC) underwent repeat echo, hemodynamic study and sacrifice 6 weeks later (9 wk TAC). Weight of mice was recorded at TAC, at three weeks and nine weeks post-TAC (in the 9 wk TAC group).

NIH-PA Author Manuscript

NIH-PA Author Manuscript

NIH-PA Author Manuscript

Definition of heart failure (HF)

HF was defined as lung/body weight > maximum value found in SHAM operated mice with remaining mice characterized as compensated LVH (21,22).

Minimally invasive transverse aortic banding (TAC)

As previously described by Hu et al (24), mice were anesthetized with ketamine (90-120 mg/kg) and xylazine (10 mg/kg) administered intraperitoneally or tribromoethanol (125-250 mg/kg intraperitoneally). A single experienced operator performed all procedures. Through a suprasternal skin incision and a mini proximal sternotomy, the thymus was retracted and the strap muscles were bluntly dissected to expose the aortic arch. A snared wire was passed underneath the aorta between the origins of the brachiocephalic and left common carotid arteries. A 6-0 silk suture was snared with the wire and pulled back around the aorta. A bent 27-gauge needle was then placed on the aortic arch; a suture was snugly tied around the needle and the aorta, followed by prompt removal of the needle. After banding, the strap muscles were approximated by a “figure of 8” suture and the skin was closed by an adhesive. Control mice were subjected to an identical procedure without placement of a ligature (SHAM).

Echocardiography

Mice underwent 2-dimensional guided M-mode echo of LV (GE Healthcare, Milwaukee, WI) with a 13 MHz linear probe under light isoflurane anesthesia (0.5-1.0%) administered via nose cone. Digital images were analyzed off-line by EchoPAC software allowing anatomic M-mode measurements. The transverse aorta was also visualized with 2-dimensional and color flow imaging. The distal transverse aortic flow velocity (distal to constriction in TAC mice) was measured by pulsed wave (PW) Doppler to assess the presence of TAC with the pressure gradient estimated using the modified Bernoulli equation (Pressure gradient = $4*\text{Velocity}^2$). Anatomic m-mode echocardiography was used to measure percent stenosis in a subset of mice with satisfactory echo images of the aortic arch (n=51). Percent stenosis was measured as the difference between the normal luminal area and the stenosed area divided by the normal luminal area. Illustrative two dimensional, color flow and PW Doppler and anatomic m mode images of the aortic arch in a SHAM and a TAC mouse are shown in Figure 1.

The LV mass and ejection fraction (EF) were calculated using the cube formula. Mid-wall fiber shortening (mFS) was calculated by the ellipsoidal two shell method.

Hemodynamics

Immediately following echo, isoflurane anesthetized mice were intubated and mechanically ventilated (Hugo Sachs Elektronik, Hugstetten, Germany). A manometer tipped catheter (Millar instruments, Houston, TX) was inserted into the LV via the right carotid artery. The LV pressure and echo measurements were used to calculate end-systolic wall stress (cESS). In a subset of animals (n=24), immediately after echo, separate manometer tipped catheters were advanced to the aorta via the right and left carotid arteries and the instantaneous (peak to peak) trans-TAC aortic pressure gradient was measured. Data analysis was performed by PVAN software (AD Instruments, Inc, Colorado Springs, CO).

Tissue harvest

Following catheterization, organs were rapidly harvested and weighed. A mid LV section preserved in 10% formalin and embedded in paraffin and cross sectioned into 5μm sections.

NIH-PA Author Manuscript

NIH-PA Author Manuscript

NIH-PA Author Manuscript

Histology and histomorphometry

LV sections were stained with picrosirius red. Interstitial fibrosis was assessed independently by a blinded experienced observer by a semi-quantitative visual analogue fibrosis scale for each quadrant of the LV, with 4 grades: 0-3 (0= No fibrosis, 1= Mild, 2=Moderate and 3=Severe fibrosis) yielding a total score between 0 and 12. Standard examples from previous studies showing each grade of fibrosis were used to enhance consistency of scoring. Given the variable peri-vascular fibrosis (within an LV section) and the variable number of vessels on any given section, analysis was focused on interstitial fibrosis remote from vessels.

Gene expression (Quantitative RT Real-Time PCR)

Total RNA was extracted from snap frozen LV tissue. RNA was reverse transcribed to cDNA by an iScript cDNA synthesis kit (Bio-Rad laboratories, Hercules, CA). cDNA was amplified and levels of gene expression were quantified by real-time quantitative PCR (TaqMan® Gene Expression Assays and Universal Probelibrary Gene Assays). Primers for ANP, and osteopontin mRNAs were used (Applied Biosystems, Foster City, CA).

Survival

Early (24 hours) and three week survival after TAC or SHAM was assessed. Survival analysis was restricted to a group of mice that were subjected to TAC during a calendar year.

Statistical Analysis

All data points as well as mean ± standard deviation are reported. Comparisons across all groups were performed by one way analysis of variance (ANOVA) followed by Bonferroni correction for multiple comparisons. Changes from three to nine weeks were assessed by paired t test. Pearson correlation was used to assess bivariate associations between continuous variables. Least squares linear regression using group as a dummy variable was used to assess differences in the relationship between variables across groups. Nominal logistic regression was used for development of the predictive model of HF. Receiver operating characteristics were used to define predictive characteristics (area under the curve, AUC) and the optimal (highest sensitivity and specificity) partition value for each predictor to distinguish mice with HF from those without HF. All analyses were 2-tailed and a p value less than 0.05 was considered statistically significant.

Results

Noninvasive in-vivo assessment of the persistence and severity of TAC

The velocity of flow in distal transverse aorta was normally distributed and < 1.0 m/sec in SHAM mice (Figure 2 A) but was not normally distributed in TAC mice (Figure 2 B). Both LV systolic pressure (Figure 2 C) and LV mass (Figure 2 D) correlated with Doppler estimated pressure gradient from the pre-cath echo performed prior to sacrifice at three or nine weeks. The invasively measured gradient correlated with Doppler estimated gradient ($n=24$, $r=0.62$, $p<0.001$) and with the severity of LVH (Figure 2 E). The percent stenosis measured with anatomic m-mode also correlated with the Doppler estimated gradient ($n=58$, $r=0.30$, $p<0.0001$) and correlated with the severity of LVH (Figure 2, F).

Cardiac structure and function at three and nine weeks post-TAC

As compared to SHAM mice, TAC mice displayed higher TA flow velocity, LV systolic pressure, chamber dimension and wall stress (Figure 3). LVH assessed by echo and at autopsy was variable but higher in TAC than SHAM mice at both three and nine weeks. EF

NIH-PA Author Manuscript

NIH-PA Author Manuscript

NIH-PA Author Manuscript

was variable, but on average was lower at both three weeks and nine weeks post-TAC. Likewise, mFS was reduced at three and nine weeks but was proportional to wall stress.

Failing versus compensated phenotype with TAC

Lung/body weights were variable but on average slightly higher than SHAM at both three and nine weeks post TAC. However, a subset of TAC mice had elevated lung weights consistent with HF, while the remaining mice had normal lung weights suggesting a compensated LVH phenotype (Figure 4). There was no difference in body weight between HF, SHAM or compensated LVH mice. Hence, we compared the characteristics of mice with compensated LVH (no pulmonary congestion) and HF (pulmonary congestion).

As compared to SHAM, the TA flow velocity was similarly elevated in compensated LVH and HF (Figure 5). The percent stenosis was higher in HF than compensated LVH mice although there was overlap between the two groups. LV systolic pressure was higher than SHAM in both groups but was lower in HF as compared to compensated LVH. Wall stress was higher than SHAM in both groups, but was higher in HF than compensated LVH (despite lower LV pressure) due to higher LV internal diameter in HF mice. LV/body weight at autopsy was higher than SHAM in both groups, but was higher in HF than compensated LVH. Indeed, the average LV/body weight was 123±54 % higher than SHAM in the HF group versus 38±7 % higher than SHAM in compensated LVH ($p<0.0001$). ANP mRNA expression was elevated in compensated LVH and was further increased in HF. Expectedly, the degree of ANP gene expression strongly correlated with the magnitude of hypertrophy (Supplemental figure 1). EF was reduced in the HF group. Both groups showed reduction in mFS and while mFS was related to wall stress in SHAM, compensated LVH and HF, this relationship was shifted downward in the HF group indicating impaired contractility. Representative LV echocardiograms from SHAM, compensated LVH and HF mice are shown in Figure 6.

The relationship between LVH (LV/body weight) and the Doppler estimated trans TAC pressure gradient (Figure 7) was shifted upward in HF mice with greater LVH for any given trans-TAC pressure gradient. A leverage point outlier resulted in non-significant slope for HF group ($R^2=0.0.4$; $p=0.33$, dotted red line). Excluding the outlier, the R^2 increased to 0.26 ($p = 0.01$, solid red line). This outlier did not affect the difference between HF and no HF groups, as the intercepts were significantly different with or without the outlier.

While both compensated LVH and HF mice had increased interstitial LV fibrosis as compared to SHAM, fibrosis was more severe in HF versus compensated LVH mice (Figure 8). Osteopontin gene expression was unchanged in compensated hypertrophy; however it was elevated 3 folds in the presence of HF and robustly correlated with the magnitude of LVH. (Supplemental figure 1).

Echocardiographic predictors of HF at three or nine weeks

Both LV mass and EF at echo conducted three weeks post-TAC accurately predicted the presence of HF at autopsy at three or nine weeks post-TAC with AUC of 0.87 and 0.84 respectively while Doppler estimated trans-TAC pressure gradient did not (Figure 9). When added to the model percent stenosis did not add further predictive information.

Interestingly, mice designated as having HF at the three week post-TAC echo displayed more severe progressive remodeling (ΔEF from three to nine weeks = -5.5±9.8%, $p=0.01$ by paired t-test) than did mice with compensated LVH (ΔEF from three to nine weeks = -1±0.1%, $p=0.13$ by paired t-test).

NIH-PA Author Manuscript

NIH-PA Author Manuscript

NIH-PA Author Manuscript

Survival

Early mortality (defined as death within 24 hours of TAC) was 45% (Figure 10). The majority of early mortality occurred at the time the ligature was tied or more commonly, after the animal had recovered from anesthesia and began to move about. A minority (< 5%) were due to operative complications (bleeding or pneumothorax). Total three week mortality was 68%.

Discussion

In this study, we defined the variability in response to TAC in male C57BL/6J mice using a 27 gauge standardizing needle for the TAC procedure. Whether studied at three or nine weeks post procedure, the presence of persistent TAC was clear with little overlap in distal TA velocity between SHAM and TAC mice. However, we found that mice subjected to TAC exhibit variable severity of perturbation in hemodynamic parameters, chamber geometry, systolic function indices and hypertrophic and fibrotic remodeling. Importantly, we describe two distinct phenotypes with TAC, compensated LVH and overt HF. While compensated LVH mice have significant LVH, the HF phenotype was constrained to mice with profound LVH and was associated with impaired contractility. Additionally, we demonstrate that reduced EF or marked increase in LV mass by echo at three weeks post-TAC can prospectively identify which mice will have a HF phenotype at autopsy, even when mice are sacrificed six weeks later. TAC is an extremely powerful experimental model. Understanding the variability involved in the model, independent of sex, strain, needle size or time course, is crucial to appropriate study design and interpretation particularly when effects of pharmacologic agents or conditional expression of genetic interventions are studied.

Variability in the murine TAC model

Review of published studies reveals variability in reported mortality, severity of LVH and presence of a failing or compensated phenotype. In male C57BL/6J mice subjected to TAC with a 27 gauge sizing needle, mortality rates <25% (16,19,25-27), 25-50% (18,20,28-30), 50-75% (31,32), or greater than 75% (8,33) have been reported although many studies do not report mortality. Similarly, in male C57/BL6 mice subjected to TAC with a 27 gauge sizing needle, reported increments in LV mass over SHAM vary from 28% to 130% at 3 weeks (15,24), and from 58% to 190% at 7-9 weeks (34,35). Studies using male C57BL/6J mice subjected to TAC with a 27 gauge sizing needle have also varied in characterizing TAC as a model of HF (6-8,10) vs compensated LVH (2-5). These differences are consistent with the variability we observed studying a large number of consecutive mice subjected to TAC with a 27 gauge sizing needle.

While strain (16), sex (17,18) and standardizing needle size (15,19,31) are well known to affect severity of remodeling with TAC, a few studies have investigated other sources of variation in the TAC model. While variable off-loading of the pressure via the right upper extremity and cranial vascular beds may contribute to variability, even ascending aortic constriction was found to produce heterogeneous responses (13). Lygate et al elegantly demonstrated band migration or internalization by serial MRI scans and proposed this as a rationalization for variable TAC remodeling (23). We too observed this on occasion but this was uncommon and did not explain the majority of the variation. Additionally, variable increases in stenosis with growth after TAC could contribute (20) although we found homogenous and relatively minor increases in body weight over the three to nine week period of observation. A recent study suggests that within an inbred strain, inherited individual variation still exists such that the parent of origin (17) may affect the response to

NIH-PA Author Manuscript

NIH-PA Author Manuscript

NIH-PA Author Manuscript

cardiac stress. We did not control for parent of origin and this may have contributed to the variation we observed.

Clearly, the severity of the stenosis will have the major effect on severity of remodeling and this may vary significantly despite the use of a standardized sizing needle owing to variation in aorta size, growth and tightness of the ligature. These factors are difficult to further standardize. Thus, studies have attempted to quantify the severity of stenosis such that the degree of remodeling can be adjusted for stenosis severity and compared between groups. Measurement of the trans-TAC gradient via catheterization of both carotid arteries, measurement of flow velocity in the right and left carotid arteries (36) or measurement of the trans-TAC Doppler velocity as used here can provide estimates of trans-stenosis pressure gradient. Each of these methods has unique strengths and limitations in terms of accuracy, feasibility and reproducibility but the non-invasive nature of Doppler estimates and ability to assess TAC severity prior to therapeutic or mechanistic interventions without compromising future vascular access is strength of this method. However, as well established in human correlates of the TAC model such as aortic stenosis, area stenosis rather than trans-stenotic pressure gradient is the preferable measure of stenosis severity as trans-stenotic pressure gradients are affected by flow and decrease in the presence of systolic dysfunction. Pressure gradients also can be variably affected by anesthetics due to effects on inotropy, vascular tone and heart rate (37). MRI provides highly reproducible anatomic information and additionally, can detect band migration. We found that anatomic m-mode imaging of the TA was feasible and identified more severe stenosis in mice with HF. However, percent stenosis was inferior to EF and severity of LVH in prospectively predicting the ultimate phenotype. Measurement of constriction area postmortem by perfusion fixation referenced to adjacent luminal area can be considered a gold standard, but is technically demanding and not available prospectively (24).

An additional source of variation is the variable hemodynamic perturbation, myocardial hypo-perfusion and myocardial damage at the time of the TAC procedure. We did not assess this factor and future studies, potentially using biomarkers of myocardial damage in the early post-TAC period may elucidate the role of acute myocardial damage in contributing to subsequent eccentric remodeling and HF despite similar chronic pressure overload.

Prospective characterization of TAC mice

The impact of genetic manipulation of fundamental signaling pathways or sarcomeric proteins is often so profound that dramatic differences in TAC-induced changes in structure and function can be confidently detected in relatively small numbers of mice - even with inherent variability resulting from TAC. However, TAC mice are increasingly being used to explore genetic interventions with more subtle effects. Most importantly, when TAC is used to test pharmacologic interventions or conditionally expressed genetic modifications after TAC, it is imperative that treated and untreated mice start from a similar baseline and that adequate numbers of mice are used as important effects may be missed or effects may appear more dramatic than truly present. Further, response to interventions may vary depending on the presence or absence of HF. Thus, we used Doppler-echo derived parameters, to both confirm and assess TAC severity as well as identify mice with or destined to develop HF after three weeks of TAC. These criteria were highly predictive of HF as defined by the presence of pulmonary congestion. This simple tool enables optimal design of therapeutic trials by randomizing mice to therapy or placebo within each phenotype (compensated versus HF) as we and others have done (13-15,25).

NIH-PA Author Manuscript

NIH-PA Author Manuscript

NIH-PA Author Manuscript

Limitations

We did not measure pre-TAC cardiac structure or function and assume a small variance of these parameters at baseline. Doppler echo is angle dependent and measured velocities may not reflect maximal instantaneous gradient. The probe used to allow high resolution 2 D images did not allow continuous wave Doppler and even the small non-imaging continuous wave probe was not highly feasible in the mouse for imaging at this site. In some mice, the velocity exceeded the Nyquist limit of the probe at the limits of the sample volume depth or size used and in these mice, the velocity could only be characterized up to 3.5 to 4.0 m/sec. However, Doppler estimated gradients did correlate with invasively measured gradients and severity of LVH. We did not correct for angle in Doppler measurements. However, this is a systematic error that may not affect the comparisons made within this experiment. We measured aortic dimensions on images collected during imaging to position PW Doppler imaging. We speculate that images obtained and optimized specifically for m-mode measurements of stenosis severity would enhance feasibility and accuracy. While we speculate that the HF phenotype is associated with neurohumoral activation, we did not measure circulating or tissue levels of neurohumoral markers. However, we saw evidence of myocardial inflammation (osteopontin). While Perrino et al (36) have elegantly demonstrated that even intermittent TAC produces activation of several pro-hypertrophic signaling cascades, differences in remodeling, systolic function and therapeutic response in compensated LVH and HF in murine models and human disease support the importance of characterization of the presence of HF in many murine studies (11-15,19,38). We have only characterized male mice of a single (but widely used) strain.

Conclusions

Murine TAC is an extremely valuable but variable animal model. Variability of response to TAC can be identified by Doppler-echo variables prospectively. These data are relevant to appropriate design of murine studies.

Supplementary Material

Refer to Web version on PubMed Central for supplementary material.

Acknowledgments

Grant Support:

This study was supported by the National Heart, Lung, and Blood Institute (HL-76611-1, HL-07111 and HL-63281).

References

1. Patten RD, Hall-Porter MR. Small animal models of heart failure: development of novel therapies, past and present. Circ Heart Fail. 2009; 2:138–44. [PubMed: 19808329]
2. Rockman HA, Ross RS, Harris AN, et al. Segregation of atrial-specific and inducible expression of an atrial natriuretic factor transgene in an in vivo murine model of cardiac hypertrophy. Proc Natl Acad Sci U S A. 1991; 88:8277–81. [PubMed: 1832775]
3. van den Bosch BJ, Lindsey PJ, van den Burg CM, et al. Early and transient gene expression changes in pressure overload-induced cardiac hypertrophy in mice. Genomics. 2006; 88:480–8. [PubMed: 16781840]
4. Izumiya Y, Shiojima I, Sato K, Sawyer DB, Colucci WS, Walsh K. Vascular endothelial growth factor blockade promotes the transition from compensatory cardiac hypertrophy to failure in response to pressure overload. Hypertension. 2006; 47:887–93. [PubMed: 16567591]

NIH-PA Author Manuscript

NIH-PA Author Manuscript

NIH-PA Author Manuscript

5. Stansfield WE, Rojas M, Corn D, et al. Characterization of a model to independently study regression of ventricular hypertrophy. J Surg Res. 2007; 142:387–93. [PubMed: 17574596]
6. Bryan PM, Xu X, Dickey DM, Chen Y, Potter LR. Renal hyporesponsiveness to atrial natriuretic peptide in congestive heart failure results from reduced atrial natriuretic peptide receptor concentrations. Am J Physiol Renal Physiol. 2007; 292:F1636–44. [PubMed: 17264312]
7. Dickey DM, Flora DR, Bryan PM, Xu X, Chen Y, Potter LR. Differential regulation of membrane guanylyl cyclases in congestive heart failure: natriuretic peptide receptor (NPR)-B, Not NPR-A, is the predominant natriuretic peptide receptor in the failing heart. Endocrinology. 2007; 148:3518–22. [PubMed: 17412809]
8. Jacobshagen C, Gruber M, Teucher N, et al. Celecoxib modulates hypertrophic signalling and prevents load-induced cardiac dysfunction. Eur J Heart Fail. 2008; 10:334–42. [PubMed: 18343721]
9. Ling H, Zhang T, Pereira L, et al. Requirement for Ca2+/calmodulin-dependent kinase II in the transition from pressure overload-induced cardiac hypertrophy to heart failure in mice. J Clin Invest. 2009; 119:1230–40. [PubMed: 19381018]
10. Faerber G, Barreto-Perreia F, Schoepe M, et al. Induction of heart failure by minimally invasive aortic constriction in mice: Reduced peroxisome proliferator-activated receptor gamma coactivator levels and mitochondrial dysfunction. J Thorac Cardiovasc Surg. 2010
11. Hunter JJ, Chien KR. Signaling pathways for cardiac hypertrophy and failure. N Engl J Med. 1999; 341:1276–83. [PubMed: 10528039]
12. Haq S, Choukroun G, Lim H, et al. Differential activation of signal transduction pathways in human hearts with hypertrophy versus advanced heart failure. Circulation. 2001; 103:670–7. [PubMed: 11156878]
13. McMullen JR, Sherwood MC, Tarnavski O, et al. Inhibition of mTOR signaling with rapamycin regresses established cardiac hypertrophy induced by pressure overload. Circulation. 2004; 109:3050–5. [PubMed: 15184287]
14. Moens AL, Takimoto E, Tocchetti CG, et al. Reversal of cardiac hypertrophy and fibrosis from pressure overload by tetrahydrobiopterin: efficacy of recoupling nitric oxide synthase as a therapeutic strategy. Circulation. 2008; 117:2626–36. [PubMed: 18474817]
15. Nagayama T, Hsu S, Zhang M, et al. Pressure-overload magnitude-dependence of the anti-hypertrophic efficacy of PDE5A inhibition. J Mol Cell Cardiol. 2008
16. Barrick CJ, Rojas M, Schoonhoven R, Smyth SS, Threadgill DW. Cardiac response to pressure overload in 129S1/SvImJ and C57BL/6J mice: temporal- and background-dependent development of concentric left ventricular hypertrophy. Am J Physiol Heart Circ Physiol. 2007; 292:H2119–30. [PubMed: 17172276]
17. Barrick CJ, Dong A, Waikel R, et al. Parent-of-origin effects on cardiac response to pressure overload in mice. Am J Physiol Heart Circ Physiol. 2009; 297:H1003–9. [PubMed: 19561308]
18. Skavdahl M, Steenbergen C, Clark J, et al. Estrogen receptor-beta mediates male-female differences in the development of pressure overload hypertrophy. Am J Physiol Heart Circ Physiol. 2005; 288:H469–76. [PubMed: 15374829]
19. Rothermel BA, Berenji K, Tannous P, et al. Differential activation of stress-response signaling in load-induced cardiac hypertrophy and failure. Physiol Genomics. 2005; 23:18–27. [PubMed: 16033866]
20. Liao Y, Ishikura F, Beppu S, et al. Echocardiographic assessment of LV hypertrophy and function in aortic-banded mice: necropsy validation. American Journal of Physiology - Heart & Circulatory Physiology. 2002; 282:H1703–8. [PubMed: 11959634]
21. Vinet L, Rouet-Benzineb P, Marniquet X, et al. Chronic doxycycline exposure accelerates left ventricular hypertrophy and progression to heart failure in mice after thoracic aorta constriction. Am J Physiol Heart Circ Physiol. 2008; 295:H352–60. [PubMed: 18487442]
22. Kiriazis H, Sato Y, Kadambi VJ, et al. Hypertrophy and functional alterations in hyperdynamic phospholamban-knockout mouse hearts under chronic aortic stenosis. Cardiovasc Res. 2002; 53:372–81. [PubMed: 11827688]
23. Lygate CA, Schneider JE, Hulbert K, et al. Serial high resolution 3D-MRI after aortic banding in mice: band internalization is a source of variability in the hypertrophic response. Basic Res Cardiol. 2006; 101:8–16. [PubMed: 16132171]

NIH-PA Author Manuscript

NIH-PA Author Manuscript

NIH-PA Author Manuscript

24. Hu P, Zhang D, Swenson L, Chakrabarti G, Abel ED, Litwin SE. Minimally invasive aortic banding in mice: effects of altered cardiomyocyte insulin signaling during pressure overload. Am J Physiol Heart Circ Physiol. 2003; 285:H1261–9. [PubMed: 12738623]
25. Divakaran V, Adrogue J, Ishiyama M, et al. Adaptive and maladptive effects of SMAD3 signaling in the adult heart after hemodynamic pressure overloading. Circ Heart Fail. 2009; 2:633–42. [PubMed: 19919989]
26. Shimura M, Minamisawa S, Takeshima H, et al. Sarcalumenin alleviates stress-induced cardiac dysfunction by improving Ca2+ handling of the sarcoplasmic reticulum. Cardiovasc Res. 2008; 77:362–70. [PubMed: 18006473]
27. Lucas JA, Zhang Y, Li P, et al. Inhibition of transforming growth factor-beta signaling induces left ventricular dilation and dysfunction in the pressure-overloaded heart. Am J Physiol Heart Circ Physiol. 2010; 298:H424–32. [PubMed: 19933419]
28. Nakamura A, Rokosh DG, Paccanaro M, et al. LV systolic performance improves with development of hypertrophy after transverse aortic constriction in mice. Am J Physiol Heart Circ Physiol. 2001; 281:H1104–12. [PubMed: 11514276]
29. Yamamoto K, Ohishi M, Katsuya T, et al. Deletion of angiotensin-converting enzyme 2 accelerates pressure overload-induced cardiac dysfunction by increasing local angiotensin II. Hypertension. 2006; 47:718–26. [PubMed: 16505206]
30. Xu X, Fassett J, Hu X, et al. Ecto-5'-nucleotidase deficiency exacerbates pressure-overload-induced left ventricular hypertrophy and dysfunction. Hypertension. 2008; 51:1557–64. [PubMed: 18391093]
31. Suryakumar G, Kasiganesan H, Balasubramanian S, Kuppuswamy D. Lack of beta3 integrin signaling contributes to calpain-mediated myocardial cell loss in pressure-overloaded myocardium. J Cardiovasc Pharmacol. 2010; 55:567–73. [PubMed: 20224428]
32. Johnston RK, Balasubramanian S, Kasiganesan H, Baicu CF, Zile MR, Kuppuswamy D. Beta3 integrin-mediated ubiquitination activates survival signaling during myocardial hypertrophy. Faseb J. 2009; 23:2759–71. [PubMed: 19364763]
33. Raher MJ, Thibault HB, Buys ES, et al. A short duration of high-fat diet induces insulin resistance and predisposes to adverse left ventricular remodeling after pressure overload. Am J Physiol Heart Circ Physiol. 2008; 295:H2495–502. [PubMed: 18978196]
34. Lei B, Chess DJ, Keung W, O'Shea KM, Lopaschuk GD, Stanley WC. Transient activation of p38 MAP kinase and up-regulation of Pim-1 kinase in cardiac hypertrophy despite no activation of AMPK. J Mol Cell Cardiol. 2008; 45:404–10. [PubMed: 18639556]
35. Takimoto E, Champion HC, Li M, et al. Oxidant stress from nitric oxide synthase-3 uncoupling stimulates cardiac pathologic remodeling from chronic pressure load. J Clin Invest. 2005; 115:1221–31. [PubMed: 15841206]
36. Perrino C, Naga Prasad SV, Mao L, et al. Intermittent pressure overload triggers hypertrophy-independent cardiac dysfunction and vascular rarefaction. J Clin Invest. 2006; 116:1547–60. [PubMed: 16741575]
37. Janssen BJ, De Celle T, Debets JJ, Brouns AE, Callahan MF, Smith TL. Effects of anesthetics on systemic hemodynamics in mice. Am J Physiol Heart Circ Physiol. 2004; 287:H1618–24. [PubMed: 15155266]
38. Li XM, Ma YT, Yang YN, et al. Downregulation of survival signalling pathways and increased apoptosis in the transition of pressure overload-induced cardiac hypertrophy to heart failure. Clin Exp Pharmacol Physiol. 2009; 36:1054–61. [PubMed: 19566828]

NIH-PA Author Manuscript

NIH-PA Author Manuscript

NIH-PA Author Manuscript

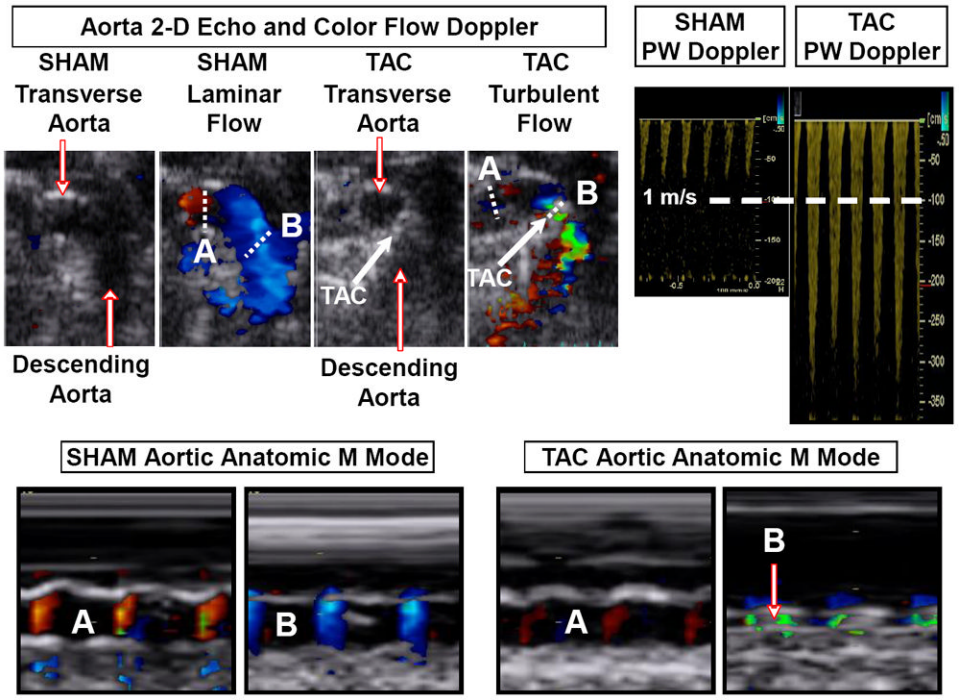

Figure 1. Representative two dimensional, anatomic m-mode and color flow and pulsed wave Doppler images of the aortic arch in a SHAM and a TAC mice

Dotted lines indicate line of interrogation for anatomic m-mode before (A) and at (B) site of SHAM or actual TAC.

NIH-PA Author Manuscript
NIH-PA Author Manuscript
NIH-PA Author Manuscript

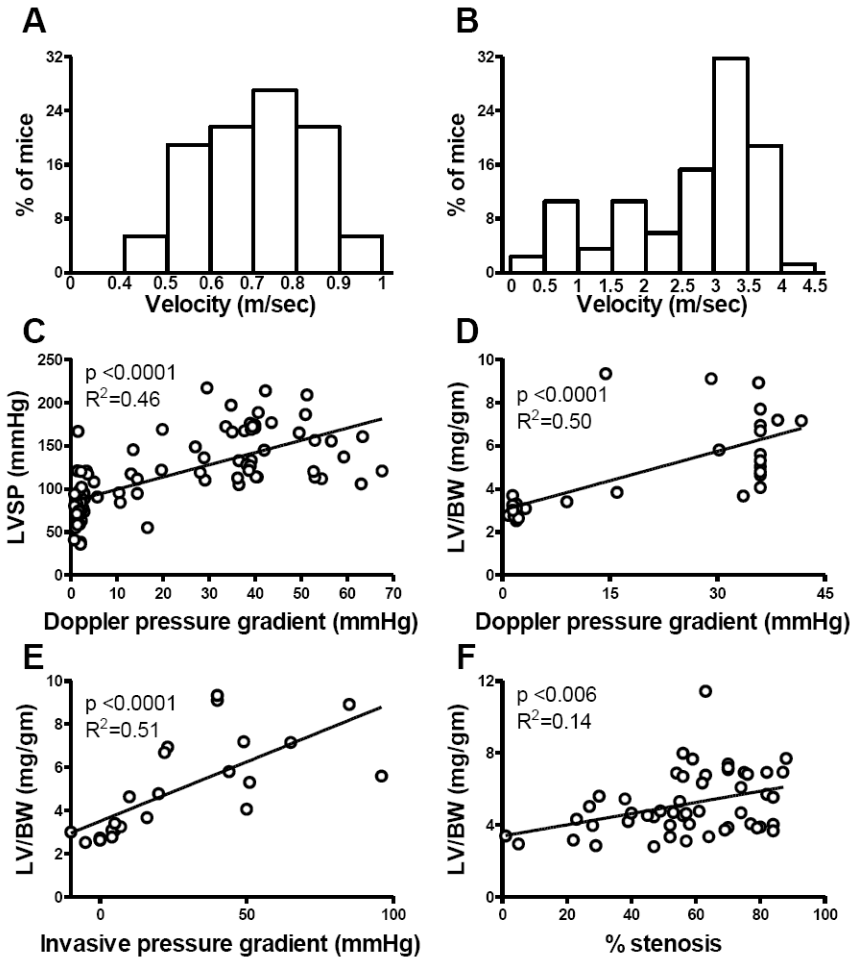

Figure 2. TAC severity

The distribution of transverse aortic flow velocity in SHAM (A) and TAC (B) mice, the correlation between Doppler derived pressure gradient and LVSP (C) and the correlations between LV/body weight measured at autopsy and Doppler estimated pressure gradient (D), invasively measured gradient (E) and anatomic m-mode estimated percent stenosis (F).

NIH-PA Author Manuscript
NIH-PA Author Manuscript
NIH-PA Author Manuscript

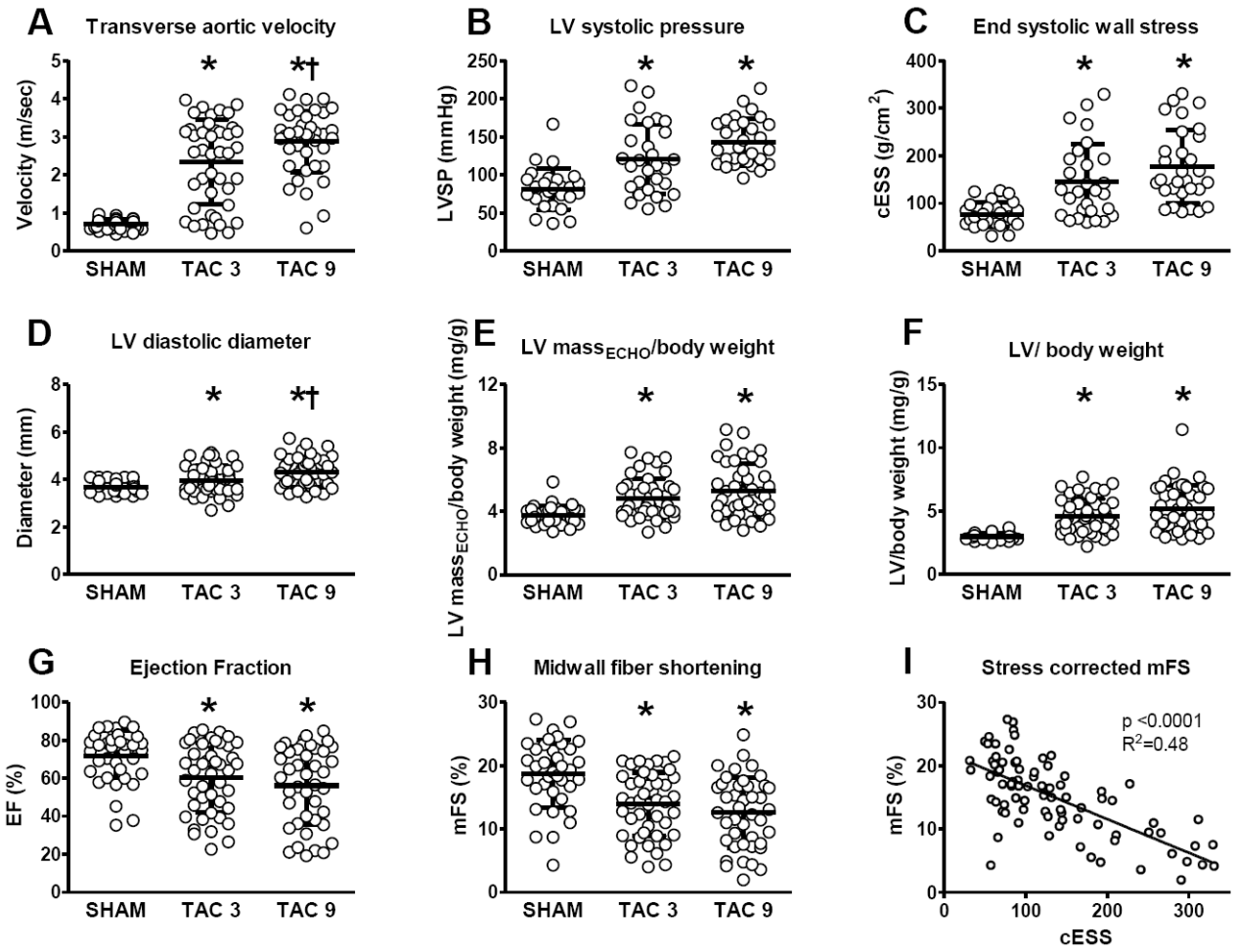

Figure 3. LV load, geometry, mass and systolic function in SHAM and 3 and 9 week TAC mice

Transverse aortic flow velocity (A), LV systolic pressure (B), end systolic wall stress (C), LV diastolic diameter (D), echo derived left ventricular mass (E), left ventricular mass at autopsy (F), ejection fraction (G), midwall fiber shortening (H) and stress corrected midwall fiber shortening (I) in SHAM and TAC groups studied at three or nine weeks. * $p < 0.05$ versus SHAM, † $p < 0.05$ versus 3 week TAC.

NIH-PA Author Manuscript

NIH-PA Author Manuscript

NIH-PA Author Manuscript

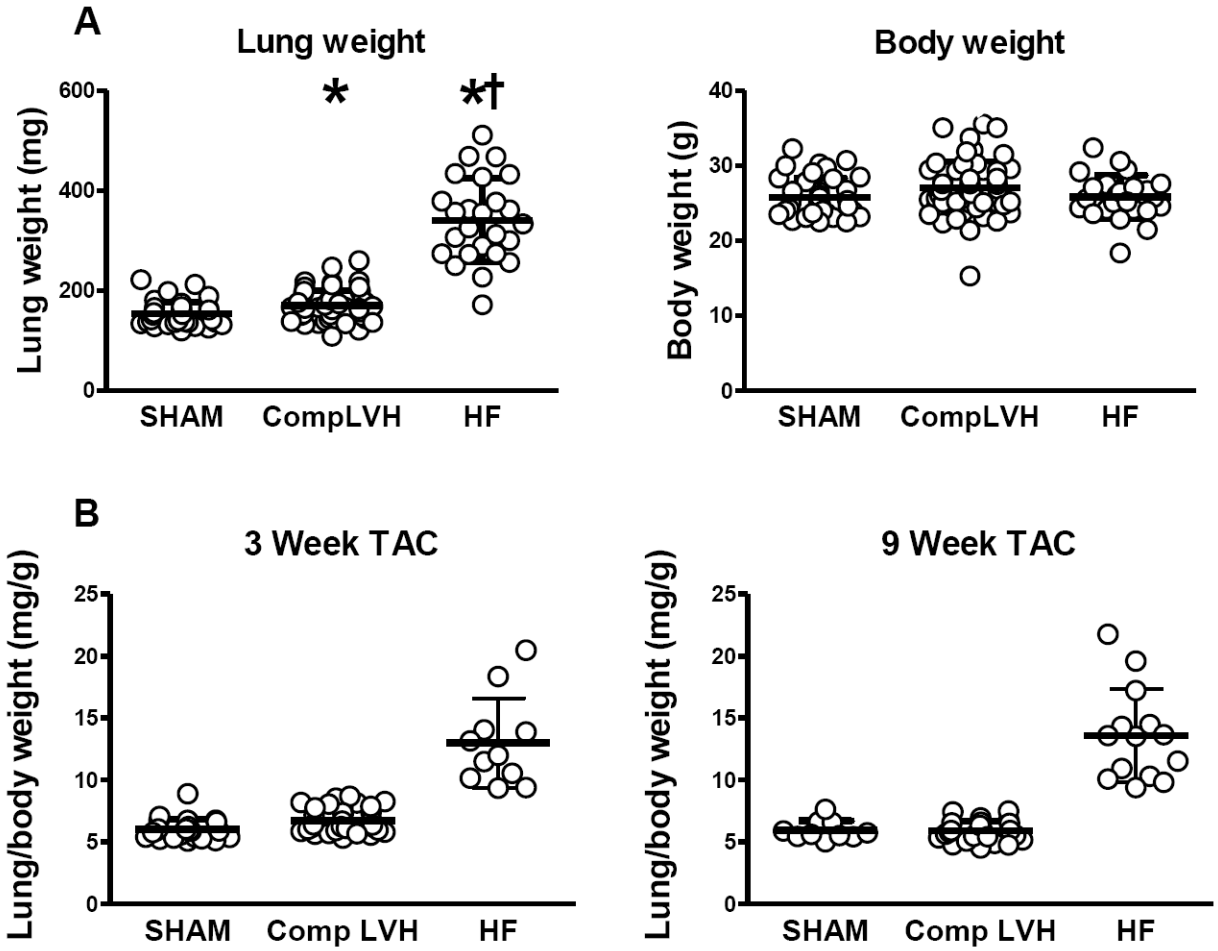

Figure 4. Development of heart failure (HF) in a subgroup of mice

Lung weight and body weight in SHAM, Compensated LVH and HF groups at three or nine weeks (A). Lung weight to body weight ratio in SHAM, Compensated LVH and HF groups at three and nine weeks post TAC (B). * $p < 0.05$ versus SHAM. † $p < 0.05$ versus compensated LVH.

NIH-PA Author Manuscript
NIH-PA Author Manuscript
NIH-PA Author Manuscript

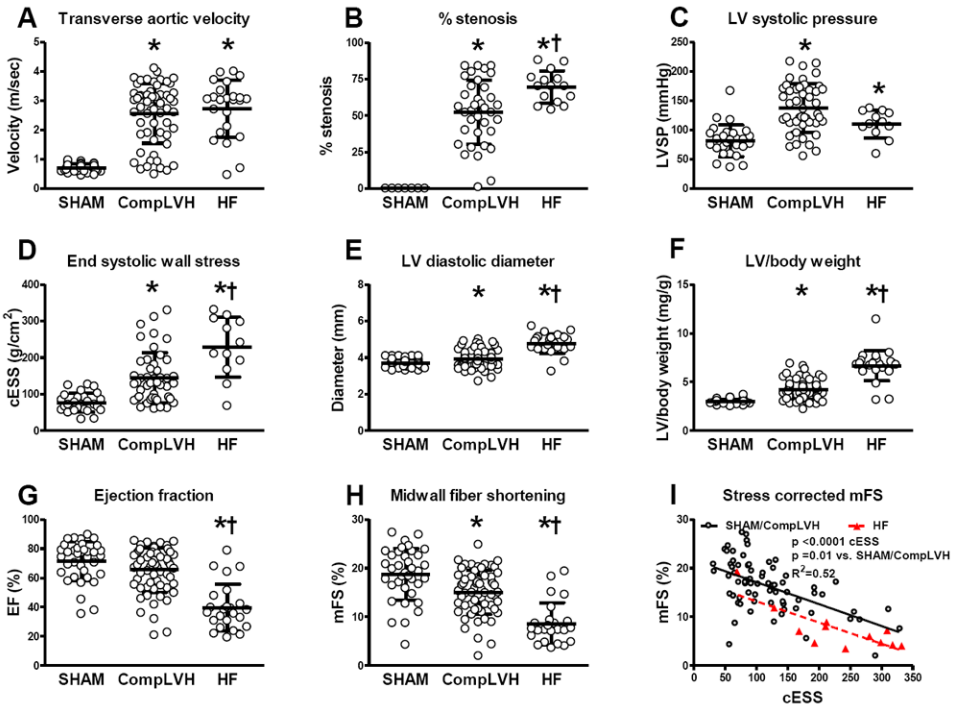

Figure 5. LV load, geometry, mass and systolic function in SHAM, compensated LVH and heart failure (HF) mice

Transverse aortic flow velocity (A), anatomic m-mode estimated percent stenosis (B), LV systolic pressure (C), end systolic wall stress (D), LV diastolic diameter (E), left ventricular mass at autopsy (F), ejection fraction (G), midwall fiber shortening (H) and stress corrected midwall fiber shortening (I) in SHAM, compensated LVH and HF mice. * $p < 0.05$ versus SHAM, † $p < 0.05$ versus compensated LVH.

NIH-PA Author Manuscript
NIH-PA Author Manuscript
NIH-PA Author Manuscript

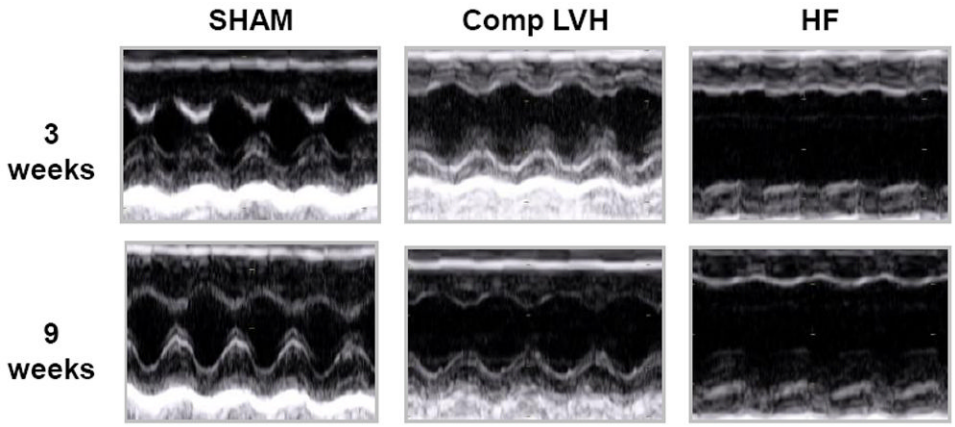

Figure 6. Representative m mode echocardiograms of SHAM, compensated LVH and heart failure (HF) mice

NIH-PA Author Manuscript

NIH-PA Author Manuscript

NIH-PA Author Manuscript

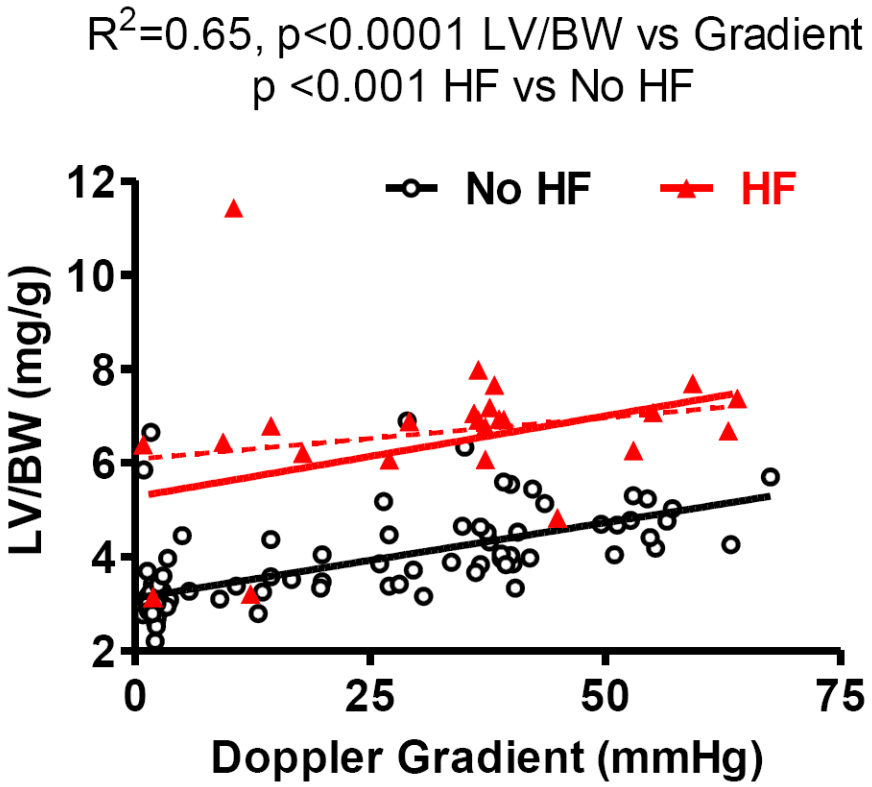

Figure 7. LV hypertrophy as a function of Doppler derived pressure gradient in heart failure (HF) and non-HF mice

At any given pressure gradient, mice with HF had a higher LV/body weight as compared with non-failing mice.

NIH-PA Author Manuscript

NIH-PA Author Manuscript

NIH-PA Author Manuscript

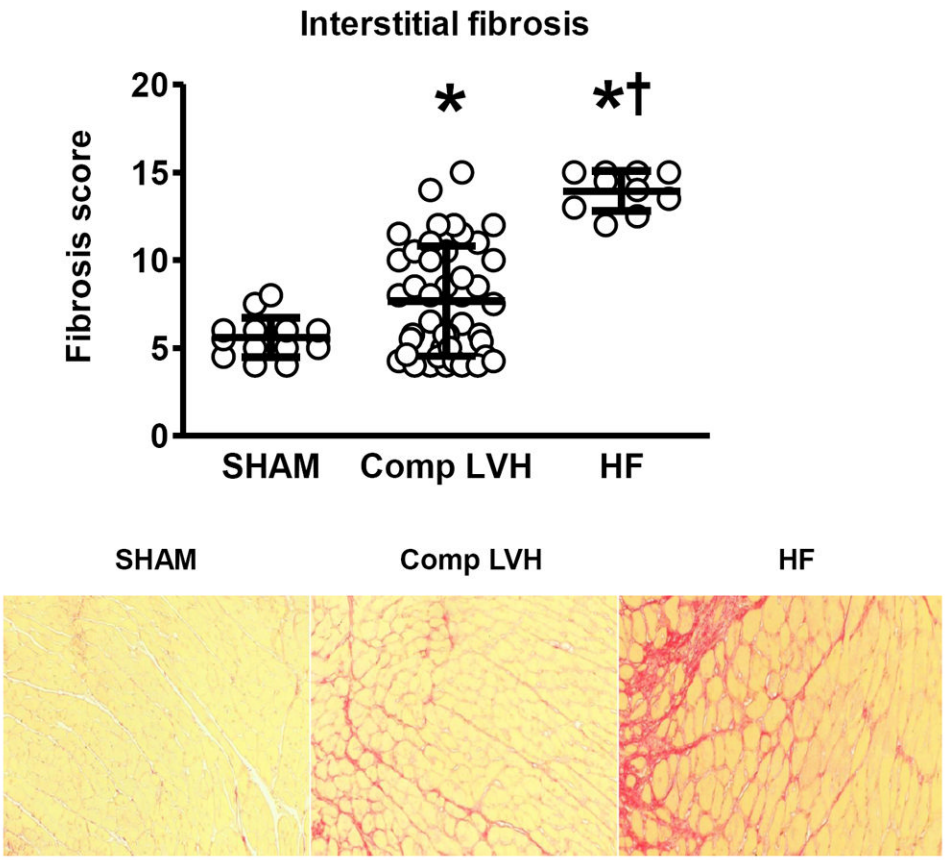

Figure 8. LV interstitial fibrosis in TAC mice

Top, fibrosis score group data in SHAM, Compensated LVH and heart failure (HF) mice. Bottom: Representative examples of peri-vascular and interstitial fibrosis in each of the three groups.

NIH-PA Author Manuscript

NIH-PA Author Manuscript

NIH-PA Author Manuscript

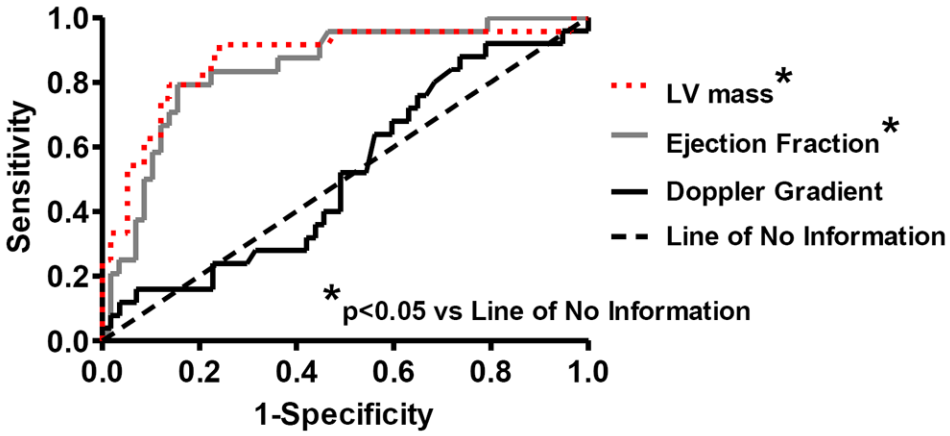

Parameter (3 wk echo)	AUC	Sensitivity	Specificity	Optimal cut-off
LV $mass_{ECHO}$	0.87	92%	76%	133 mg
Ejection Fraction	0.84	79%	84%	50%
Doppler Gradient	0.52	88%	26%	12 mmHg

Figure 9. Receiver operating characteristic curves of echocardiographic predictors of HF at autopsy

The area under curve, with the optimal cutoff value, sensitivity and specificity is shown for each variable obtained at the three week echo.

NIH-PA Author Manuscript

NIH-PA Author Manuscript

NIH-PA Author Manuscript

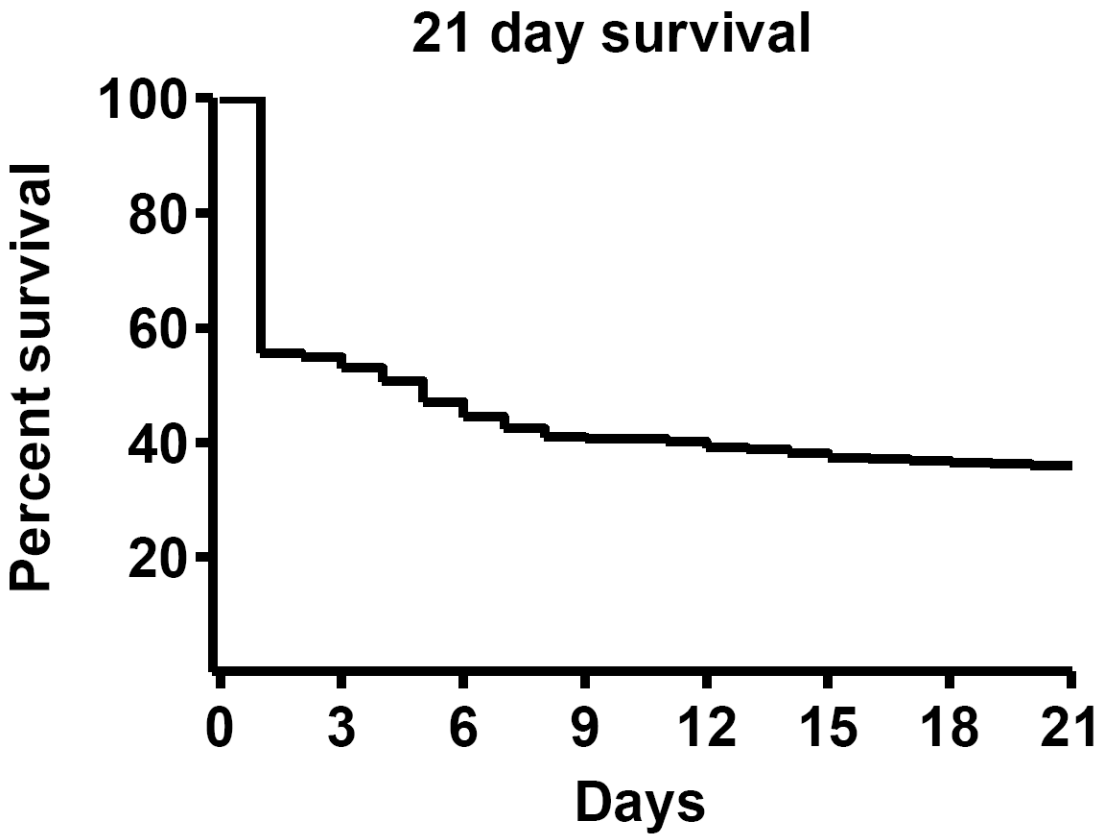

Figure 10. Kaplan-Meier survival curve in TAC mice

21 day survival including operative mortality. Number at risk = 390 (died = 244; survived = 140).